

Tailoring electromagnetically induced transparency effect of terahertz metamaterials on ultrathin substrate

Yonggang ZHANG^{1,2}, Jingbo WU^{1,3*}, Lanju LIANG¹, Gaochao ZHOU¹,
Fan ZHENG¹, Chun LI¹, Caihong ZHANG¹ & Biaobing JIN^{1*}

¹Research Institute of Superconductor Electronics, School of Electronic Science and Engineering, Nanjing University, Nanjing 210093, China;

²School of Electrical and Information Engineering, Anhui University of Science and Technology, Huainan 232001, China;

³School of Electronic and Electrical Engineering, University of Leeds, Leeds LS2 9JT, United Kingdom

Received November 4, 2015; accepted December 18, 2015; published online February 25, 2016

Abstract Electromagnetically induced transparency (EIT) is a fascinating phenomenon in optical physics and has been employed in slow light technology. In this work, we use terahertz (THz) metamaterials to mimic EIT phenomenon and study their spectral dependence on the coupling strength between bright and dark resonators. In these metamaterials, two kinds of resonators are located on two different layers separated by a 10- μm -thick polyimide (PI) film. The whole sample is supported by a 5- μm -thick flexible PI film, so the Fabry-Perot resonance at THz can be avoided. The coupling strength is tuned by the translational offset of symmetry axes between two different kinds of resonators, resulting in the change of EIT-like spectra.

Keywords metamaterials, EIT, flexible, ultrathin substrate, equivalent conductivity

Citation Zhang Y G, Wu J B, Liang L J, et al. Tailoring electromagnetically induced transparency effect of terahertz metamaterials on ultrathin substrate. *Sci China Inf Sci*, 2016, 59(4): 042414, doi: 10.1007/s11432-016-5537-5

1 Introduction

Electromagnetically induced transparency (EIT) is a quantum mechanical process observed in specific three-level atomic system, which produces an extremely-narrow transparent window with low absorption and steep dispersion in an opaque medium [1–6]. The extreme dispersion of the EIT can reduce the group velocity of light by 7 orders in magnitude [6] and store light temporally [7–9]. Moreover, the narrow window can provide a well-defined frequency marker for precision measurement [10]. However, the disadvantages of the atomic EIT system are also obvious. The EIT is only applicable in some specific atomic systems and rigorous experimental environment. Besides that, the frequency window is fixed by the energy levels of atomic transitions in the visible region [10]. The experimental complications and the limited spectrum range have significantly obstructed its fundamental research and practical applications.

* Corresponding author (email: jbwu84@gmail.com, bbjin@nju.edu.cn)

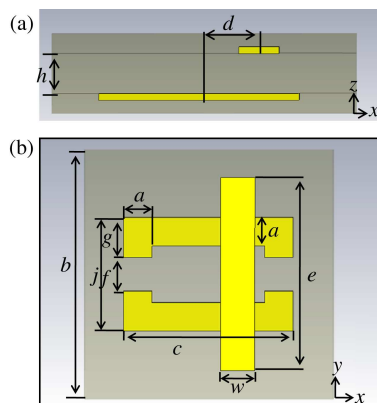


Figure 1 (Color online) Schematic representation of unit cell of THz EIT metamaterials. (a) Top view of the structure. The translational offset between the centers of dark resonator and radiative resonator is denoted by d . (b) Front view of the structure. The periodicity of the unit cell is $b = 220 \mu\text{m}$. Feature sizes are $a = 20 \mu\text{m}$, $c = 150 \mu\text{m}$, $e = 180 \mu\text{m}$, $f = 40 \mu\text{m}$, $g = 30 \mu\text{m}$, $j = 100 \mu\text{m}$, $w = 30 \mu\text{m}$ and $h = 10 \mu\text{m}$.

To take advantage of the EIT effect, the EIT phenomenon has been mimicked by solid-state, on-chip all optical and optomechanic systems [11–13]. In the past decade, metamaterials which are artificial electromagnetic structures provided an excellent platform to study EIT effect from microwave to visible light region [14–35]. Using metamaterials to mimic EIT phenomenon was first proposed by Zhang et al. [14]. A typical unit cell of EIT metamaterials includes two coupled resonators with different quality factors. Only the resonator with lower quality factor can couple to the free space radiation directly, so it is called bright resonator. Another one is dark resonator as it cannot be directly excited by incident wave. For THz EIT metamaterials, the bright and dark resonators are usually fabricated onto a thick and rigid substrate, e.g. 0.5-mm-thick silicon or MgO substrates. The Fabry-Perot (F-P) resonance frequency in such thick substrate is located at THz frequency range, which could interfere with the spectral response of metamaterials [36–38]. In this work, we characterized THz EIT metamaterials fabricated on ultrathin substrates. This metamaterial with ultrathin substrate is more close to the practical situation than those on thick substrates. Therefore, the physical properties obtained from this EIT structure will be more valuable. In addition, the ultrathin substrate made from polyimide (PI) is flexible, making the devices convenient to be attached on arbitrary surface. This is not affected by the incident electromagnetic wave which is perpendicular to the direction of the structure.

In our design, the bright and dark resonators are on the different layers which are separated by a dielectric layer. The coupling strength can be easily tuned by the relative displacement of their symmetry axes. From the measured and simulated spectra, the coupling strength is extracted.

2 Design and fabrication

The structure of a unit cell is shown in Figure 1. Each unit cell consists of two resonators, which are located at different layers. The straight metallic strip near the top works as bright resonator, it couples to the incident THz wave directly. The dark resonator is double-gap split ring resonator (DSRR) onto the bottom substrate. The isolating layer between two layers of metal resonators is a 10- μm -thick PI film. The top and bottom layers are 5- μm -thick PI films. The incident electromagnetic (EM) wave is normal to the plane of the metamaterial (z -axis) with polarization along y -direction.

For the fabrication of device, first, a 5- μm -thick PI film is formed onto the silicon wafer by spin coating and baking. Second, a 200-nm-thick gold layer is deposited on this PI layer using thermal evaporation and the dark resonators are patterned using conventional photolithography. Third, a 10- μm -thick PI film is formed by spin coating and baking. Another 200-nm-thick gold layer is deposited to form the bright resonator. Using alignment marks at the edge of the mask, the different translational offset d between symmetry axes of resonators is obtained. Fourth, the top PI layer with a 5- μm thickness is spin-coated.

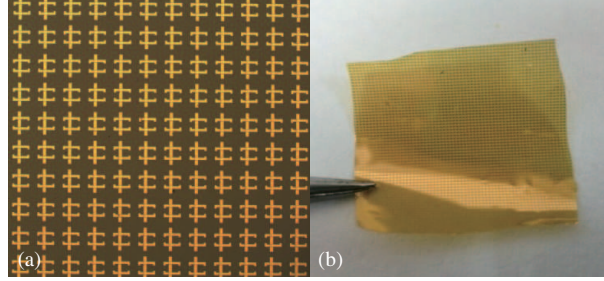


Figure 2 (Color online) Microscopic (a) and optical (b) images of the fabricated EIT metamaterials ($d = 30 \mu\text{m}$).

Finally, the whole structure is peeled off from the silicon wafer. The microscopic and optical images of samples are shown in Figure 2(a) and (b) respectively.

3 Results and discussion

Figure 3(a) and (b) show the simulated and measured transmission spectra for different d respectively. In Figure 3(a), when $d = 0 \mu\text{m}$, only one resonant dip is observed in the transmission spectra, indicating that there is not EIT spectral response. As d is increased to $5 \mu\text{m}$, there is a protrusion on the right side of transmission dip. A typical characteristic of the EIT is observed when $d = 7.5 \mu\text{m}$. The maximum transmittance of the transparency window gradually increases with increasing d .

The condition for realizing EIT in metamaterials is the creation of destructive interference of two different modes having the same resonance frequencies [24]. When $d = 0 \mu\text{m}$, the structure is symmetrical, so destructive interference is not supported. When d is increased to $5 \mu\text{m}$, the symmetry of structure is destroyed and destructive interference occurs, and the EIT phenomenon therefore appears. The transparency window can be seen from the spectrum of offset $d = 5 \mu\text{m}$ although it is very weak. With the increase of d , the asymmetry of the structure enhances and coupling effect becomes stronger, the transmittance peak gradually increases.

We also characterized the samples utilizing THz time-domain spectroscopy (THz-TDS). The measured spectra shown in Figure 3(b) agree very well with the simulation results. The evolution of the transmission spectra from single resonance to EIT response are clearly displayed both theoretically and experimentally. A trivial difference between them lies in the fact that the transmission magnitudes in the simulation are 2–3 dB larger than the experimental results. The additional loss for measurement may be attributed to some minor defects that are present in metallic structures and polyimide films and the curvature of the sample.

Figure 4 shows the group delay at different d . When $d = 12.5 \mu\text{m}$, we get the maximum value of about 5 ps. With the increase of d , the corresponding group delay-bandwidth increases, it is mainly attributed to the increase of the coupling coefficient.

The equations describing the EIT with two coupled resonators are as follows [34,35]:

$$\frac{1}{\omega_1^2} \frac{\partial^2 p}{\partial t^2} + \frac{r_1}{\omega_1} \frac{\partial p}{\partial t} + p = f - \kappa q, \quad (1)$$

$$\frac{1}{\omega_2^2} \frac{\partial^2 q}{\partial t^2} + \frac{r_2}{\omega_2} \frac{\partial q}{\partial t} + q = -\kappa p, \quad (2)$$

where ω_1 , ω_2 and γ_1 , γ_2 are the resonance frequencies and damping factors of bright and dark resonators respectively, $p(t)$ and $q(t)$ represent the excitation in bright and dark resonators respectively, $f(t)$ is the external radiation applied on the bright resonator, κ is the coupling coefficient of two resonators. The key element of classical EIT system is described by Eqs. (1) and (2) and EIT spectral response can be obtained using this model. However, the shortage of this model lies in that some essential parameters of EIT system (e.g. group delay) cannot be extracted using it.

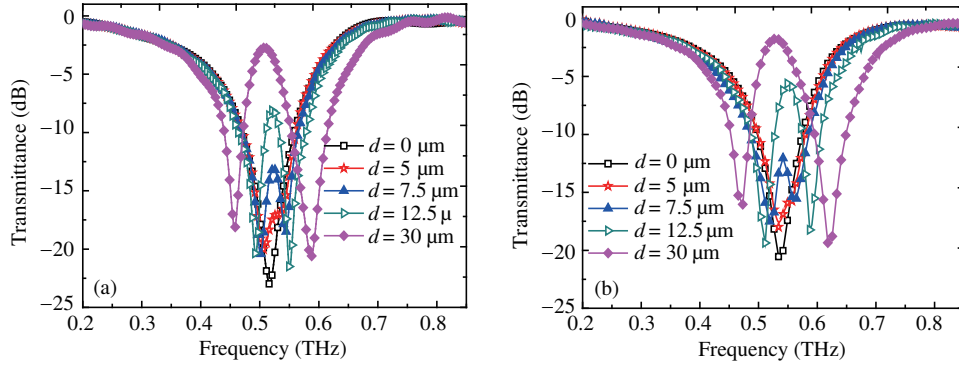


Figure 3 (Color online) (a) Simulated transmission spectra of the EIT metamaterials with different d ; (b) the corresponding measured spectra.

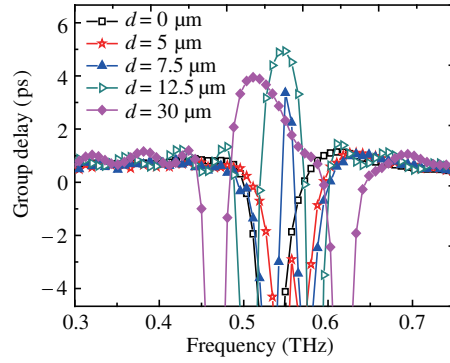


Figure 4 (Color online) Calculated group delay spectra of samples from the measured transmission spectra.

If the thickness of metamaterials is much lower than free space wavelength, we can use an equivalent current sheet with surface conductance of σ to describe its response to external radiation. The scattering parameters of an electric current sheet are [34,39]

$$T = \frac{2}{2 + \xi\sigma}, \quad (3)$$

where T is transmission coefficient, ξ is the wave impedance of external waves. From theoretical model, the surface conductivity σ can be expressed as follows [34,39]:

$$\sigma \approx -i\omega \frac{\beta D_2(\omega)}{D_1(\omega)D_2(\omega) - \kappa^2}, \quad (4)$$

where

$$D_1(\omega) = 1 - (\omega/\omega_1)^2 - i\gamma_1(\omega/\omega_1), \quad (5)$$

$$D_2(\omega) = 1 - (\omega/\omega_2)^2 - i\gamma_2(\omega/\omega_2), \quad (6)$$

β is static surface susceptibility.

Considering the thickness PI layer between two metallic layers is only 10 μm , far below the free space THz wavelength, so they can still be viewed as a layer of conducting film. Here, the equivalent surface conductivity σ of conducting film, which is used to quantize the interaction of incident wave with the equivalent medium, can be retrieved from the transmission spectra. Using Eq. (3), the equivalent surface conductivity of samples with different d were obtained (see Figure 5). When $d \neq 0$ μm , a sharp incision appears in the spectra of equivalent conductivity. With the increase of d , the incision peak becomes larger and its width becomes broader.

The coupling coefficients were obtained from equivalent surface conductivity by fitting. As shown in Figure 6, when $d = 0$ μm , the coupling coefficient $\kappa = 0$, indicating that destructive interference does not occur. When $d \neq 0$, structural symmetry is broken. In that case, the destructive interference appears, so there is coupling interaction between the two resonators ($\kappa > 0$). As d is increased, κ also increases.

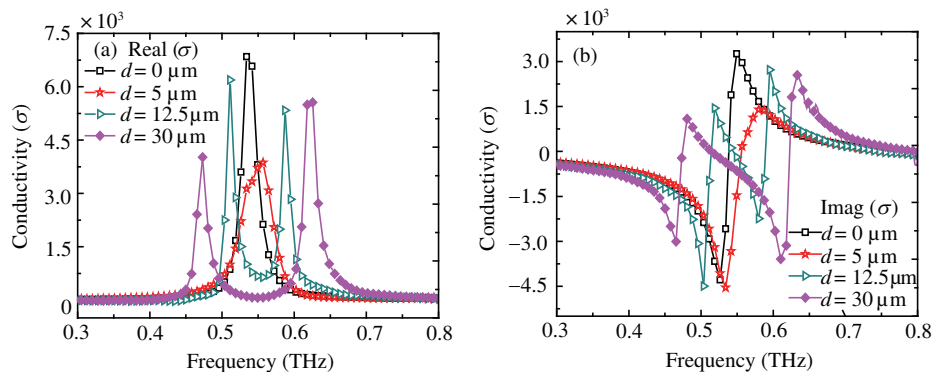


Figure 5 (Color online) Equivalent surface conductivity (unit is S) with different offset d , (a) Real (σ); (b) Image (σ).

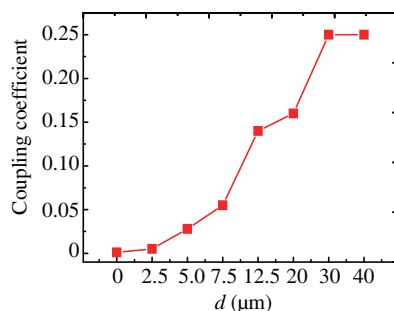


Figure 6 (Color online) Coupling coefficients for different d .

4 Conclusion

In conclusion, we demonstrated THz EIT metamaterials fabricated on ultrathin and flexible substrates both theoretically and experimentally. By changing the relative translational displacement of bright and dark resonators on different layers, the EIT response is introduced and then tuned, which is well explained by the change of coupling strength. These results show good prospects of THz metamaterials in applications such as slowing down THz wave and biosensor.

Acknowledgements This work was supported by National Basic Research Program of China (Grant Nos. 2011CBA00107, 2014CB339800), National Natural Science Foundation of China (Grant Nos. 60990322, 61071009, 61027008, 61007034), Key Programs of Natural Science Foundation of Higher Education Institution of Anhui Province, Priority Academic Program Development of Jiangsu Higher Education Institutions (PAPD), and Jiangsu Provincial Key Laboratory of Advanced Manipulating Technique of Electromagnetic Wave.

Conflict of interest The authors declare that they have no conflict of interest.

References

- Harris S E. Electromagnetically induced transparency. *Phys Today*, 1997, 50: 36–42
- Fleischhauer M, Imamoglu A, Marangos J P. Electromagnetically induced transparency: optics in coherent media. *Rev Mod Phys*, 2005, 77: 633–673
- Yin X G, Feng T H, Yip S P, et al. Tailoring electromagnetically induced transparency for terahertz metamaterials: from diatomic to triatomic structural molecules. *Appl Phys Lett*, 2013, 103: 021115
- Jing H H, Zhu Z H, Zhang X Q, et al. Plasmon-induced transparency in terahertz metamaterials. *Sci China Inf Sci*, 2013, 56: 120406
- Liu X J, Han J G, Zhang W L, et al. Electromagnetically induced transparency in terahertz plasmonic metamaterials via dual excitation pathways of the dark mode. *Appl Phys Lett*, 2012, 100: 131101
- Hau L V, Harris S E, Dutton Z, et al. Light speed reduction to 17 metres per second in an ultracold atomic gas. *Nature*, 1999, 397: 594–598
- Liu C, Dutton Z, Behroozi C H, et al. Observation of coherent optical information storage in an atomic medium using halted light pulsed. *Nature*, 2001, 409: 490–493

- 8 Bajcsy M, Zibrov A S, Lukin M D. Stationary pulses of light in an atomic medium. *Nature*, 2003, 426: 638–641
- 9 Phillips D F, Fleischhauer A, Mair A, et al. Storage of light in atomic vapor. *Phys Rev Lett*, 2001, 86: 783–786
- 10 Boyd R W, Gauthier D J. Photonics: transparency on an optical chip. *Nature*, 2006, 441: 701–702
- 11 Bigelow M S, Lepeshkin N N, Boyd R W. Superluminal and slow light propagation in a room-temperature solid. *Science*, 2003, 301: 200–202
- 12 Xu Q F, Sandhu S, Povinelli M L, et al. Experimental realization of an on-chip all-optical analogue to electromagnetically induced transparency. *Phys Rev Lett*, 2006, 96: 123901
- 13 Safavi-Naeini A H, Chan J, Eichenfield M, et al. Electromagnetically induced transparency and slow light with optomechanics. *Nature*, 2011, 472: 69–73
- 14 Zhang S, Genov D A, Wang Y, et al. Plasmon-induced transparency in metamaterials. *Phys Rev Lett*, 2008, 101: 047401
- 15 Singh R, Rochstuhl C, Lederer Falk, et al. Coupling between a dark and a bright eigenmode in a terahertz metamaterial. *Phys Rev B*, 2009, 79: 085111
- 16 Zheludev N I, Kivshar Y S. From metamaterials to metadevices. *Nat Mater*, 2012, 11: 917–924
- 17 Liu Y M, Zhang X. Metamaterials: a new frontier of science and technology. *Chem Soc Rev*, 2011, 40: 2494–2507
- 18 Tao H, Padilla W J, Zhang X, et al. Recent progress in electromagnetic metamaterial devices for terahertz applications. *IEEE J Sel Top Quan Elect*, 2011, 17: 92–101
- 19 Zhang L, Tassin P, Koschny T, et al. Large group delay in a microwave metamaterial analog of electromagnetically induced transparency. *Appl Phys Lett*, 2010, 97: 241904
- 20 Chowdhury D R, Singh R, Taylor A J, et al. Ultrafast manipulation of near field coupling between bright and dark modes in terahertz metamaterial. *Appl Phys Lett*, 2013, 102: 011122
- 21 Singh R, Al-Naib I A I, Koch M, et al. Observing metamaterial induced transparency in individual Fano resonators with broken symmetry. *Appl Phys Lett*, 2011, 99: 201107
- 22 Gu J Q, Singh R, Liu X J, et al. Active control of electromagnetically induced transparency analogue in terahertz metamaterials. *Nat Comm*, 2012, 3: 1151
- 23 Wu J B, Wan J, Liang L J, et al. Superconducting terahertz metamaterials mimicking electromagnetically induced transparency. *Appl Phys Lett*, 2011, 99: 161113
- 24 Jin B B, Wu J B, Zhang C H, et al. Enhanced slow light in superconducting electromagnetically induced transparency metamaterials. *Supercond Sci Tech*, 2013, 26: 074004
- 25 He Y R, Zhou H, Jin Y, et al. Plasmon induced transparency in a dielectric waveguide. *Appl Phys Lett*, 2011, 99: 043113
- 26 Meng F Y, Wu Q, Erni D, et al. Polarization-independent metamaterial analog of electromagnetically induced transparency for a refractive-index-based sensor. *IEEE T Microw Theory*, 2012, 60: 3013–3022
- 27 Zhu L, Meng F Y, Fu J H, et al. An electromagnetically induced transparency metamaterial with polarization insensitivity based on multi-quasi-dark modes. *J Phys D Appl Phys*, 2012, 45: 445105
- 28 Zhu L, Meng F Y, Wu Q, et al. Multi-band slow light metamaterial February. *Opt Express*, 2012, 20: 4494–4502
- 29 Li H M, Liu S B, Liu S Y, et al. Electromagnetically induced transparency with large group index induced by simultaneously exciting the electric and the magnetic resonance. *Appl Phys Lett*, 2014 105: 133514
- 30 Tan W, Sun Y, Wang Z G, et al. Manipulating electromagnetic responses of metal wires at the deep subwavelength scale via both near- and far-field couplings. *Appl Phys Lett*, 2014, 104: 091107
- 31 Li H M, Liu S B, Liu S Y, et al. Low-loss metamaterial electromagnetically induced transparency based on electric toroidal dipolar response. *Appl Phys Lett*, 2015, 106: 083511
- 32 Li H M, Liu S B, Liu S Y, et al. Electromagnetically induced transparency with large delay-bandwidth product induced by magnetic resonance near field coupling to electric resonance. *Appl Phys Lett*, 2015, 106: 114101
- 33 Tassin P, Zhang L, Economou E N, et al. Low-loss metamaterials based on classical electromagnetically induced transparency. *Phys Rev Lett*, 2009, 102: 053901
- 34 Tassin P, Zhang L, Zhao R, et al. Electromagnetically induced transparency and absorption in metamaterials: the radiating two-oscillator model and its experimental confirmation. *Phys Rev Lett*, 2012, 109: 187401
- 35 Garrido C L, Martinez M A, Nussenzeig P. Classical analog of electromagnetically induced transparency. *Am J Phys*, 2002, 70: 37–41
- 36 Zhang Y G, Wu J B, Liang L J, et al. Effect of loss and coupling on the resonance of metamaterial: an equivalent circuit approach. *Sci China Inf Sci*, 2014, 57: 122401
- 37 Jin B B, Zhang C H, Shen X F, et al. Extraction of material parameters of a bi-layer structure using Terahertz time-domain spectroscopy. *Sci China Inf Sci*, 2014, 57: 082408
- 38 Liang L J, Jin B B, Wu J B, et al. Terahertz narrow bandstop, broad bandpass filter using double-layer S-shaped metamaterials. *Sci China Inf Sci*, 2013, 56: 120412
- 39 Tassin P, Koschny T, Soukoulis C M. Effective material parameter retrieval for thin sheets: theory and application to graphene, thin silver films, and single-layer metamaterials. *Phys B*, 2012, 407: 4062–4065